Hindawi
Shock and Vibration
Volume 2020, Article ID 3069895, 12 pages
https://doi.org/10.1155/2020/3069895

Research Article

Modeling of Vibration Condition in Flat Surface Grinding Process

Amon Gasagara,[1] **Wuyin Jin**,[1,2] **and Angelique Uwimbabazi**[1]

[1]*School of Mechanical and Electronic Engineering, Lanzhou University of Technology, Lanzhou 730050, Gansu, China*
[2]*Key Laboratory of Digital Manufacturing Technology and Application, Ministry of Education, Lanzhou University of Technology, Lanzhou 730050, Gansu, China*

Correspondence should be addressed to Wuyin Jin; wuyinjin@hotmail.com

Received 7 November 2019; Revised 27 December 2019; Accepted 16 January 2020; Published 10 February 2020

Academic Editor: Davood Younesian

This article presents a new model of the flat surface grinding process vibration conditions. The study establishes a particular analysis and comparison between the influence of the normal and tangential components of grinding forces on the vibration conditions of the process. The bifurcation diagrams are used to examine the process vibration conditions for the depth of cut and the cutting speed as the bifurcation parameters. The workpiece is considered to be rigid and the grinding wheel is modeled as a nonlinear two-degrees-of-freedom mass-spring-damper oscillator. To verify the model, experiments are carried out to analyze in the frequency domain the normal and tangential dynamic grinding forces. The results of the process model simulation show that the vibration condition is more affected by the normal component than the tangential component of the grinding forces. The results of the tested experimental conditions indicate that the cutting speed of 30 m/s can permit grinding at the depth of cut up to 0.02 mm without sacrificing the process of vibration behavior.

1. Introduction

Grinding is a type of abrasive machining process which is very important in manufacturing. It is a complex material cutting, in which the cutting action is accomplished by sharp abrasive grit bonded together by an appropriate bonding material and distributed randomly to make the shape of an abrasive tool according to the requirements of the application. The grits cut metallic and nonmetallic workpieces and remove material in the form of chips to make the surface flat or smoother. The flat surface grinding process is used to generate a smooth surface finish on flat surfaces. It uses a surface grinder machine and an abrasive rotating wheel to smoothen the flat surface of the workpiece to attain the desired surface according to a functional purpose. The workpiece material is held using a chuck laid on a reciprocating or rotating table. The ferromagnetic workpiece is clamped by a magnetic chuck, although nonferromagnetic workpiece is clamped by machine vice or by vacuum.

However, the flat surface grinding process is a complex phenomenon with several nonlinear characteristics that influence each other. The complexity lies in the mode of interaction between the grinding wheel and the workpiece which generates the heat [1, 2] and grinding forces [3, 4] to induce the vibration of the process which significantly affects the quality of the grounded workpiece. Grinding forces are classified according to the interaction mechanism in the wheel-workpiece contact zone such as chip formation forces, friction force, and plowing force, respectively. The plowing forces are very small compared to other forces and can be negligible for mathematical and theoretical model simplification. In his model, Malkin [5] subdivided the total grinding forces into two components, which are cutting force and frictional force. The cutting force was further subdivided into two components, namely, chip formation force and plowing force. Compared with chip formation force, plowing force was significantly less and was ignored, and the total grinding force is a summation of chip formation force and friction force in normal and tangential directions, respectively.

Theoretical models have significantly accelerated the analysis and understanding of the surface grinding process

and have reduced the time and cost of experimental procedures. Since the last decades, dynamic analysis and force modeling of the surface grinding process have been areas of research interest for researchers [6–9]. The need for developing a clear and proper comprehension of the process has led to several recognized forces and vibration models that are available today in the literature. Tang et al. [10] developed a mathematical model to calculate the chip formation forces, taking into account the relationship between chip formation energy and chip formation force, and considered the influence of process parameters on friction coefficient to calculate the sliding force. The research elaborated a formula for grinding forces calculation in surface grinding process. Durgumahanti et al. [11] established a grinding force model considering the three stages of wheel-workpiece contact zone, frictional coefficient variation, and process parameters; unlike the previous models in which it was considered to be a constant, the results reveal that the coefficient of friction changes with the parameters of the process. Chang and Wang [12] considered the single grit force as a function of grits distributed randomly on the rotating wheel. The results showed that the grit density function varies proportionally compared to the average number of grits per unit area and the grinding force increases with the increase in grinding width and the depth of cut.

Mishra and Salonitis [13] modified and validated Werner's model of grinding forces by considering the material of the workpiece, the parameter of the process, and the auxiliary equipment. The research provided a simple and accurate model able to determine grinding forces in advanced grinding. Salonitis et al. [14] studied the effect of the process parameters and wheel characteristics on grinding forces during grind-hardening process. The results showed that increase of the depth of cut and the speed of the workpiece lead to an increase of cutting forces. Besides the use of finer grits, harder grade and denser structure grinding wheel result in increase of grinding forces. Jiang et al. [15] modeled the microscopic interaction between the workpiece and the grinding wheel, taking into account the parameters such as topography of the grinding wheel, the distribution of grain, and the mechanical properties of the workpiece which were not integrated in the previous models. The results demonstrated the process of grinding force generation and the heat partition in the grinding system. Liu et al. [16] used the empirical approach based on parameters like grinding wheel diameter, cutting speed, the depth of cut, and the feed rate for grinding forces measurement; the approach enabled the understanding of grinding force signal processing and the grinding fixture design. Wang et al. [17] presented a method for surface formation in rotary ultrasonic grinding of brittle and hard materials. The results showed that the grinding force is proportional to the feed rate and the depth of cut. Wang et al. [18] studied the effect of grinding force and grinding heat on the face gear in grinding with the disk wheel having a long radius. The study established a thermomechanical coupling and a strain-stress model of the face gear. Zhu et al. [19] developed a model of material removal mechanism in grinding process considering the microscopic grit-workpiece interaction. The proposed model was able to predict the relationship between force-depth of cut and wear of the individual cutting grit and reported the framework of modeling the compliant grinding process which was not reported in the previous models.

Yuqin et al. [20] studied a model for surface roughness in ultrasonic-assisted grinding based on the contact analysis. The results showed that the workpiece surface roughness increases with the increase of the depth of cut and the workpiece surface roughness increases and then decreases with the increase of ultrasonic amplitude. Zhao et al. [21] investigated the effect of grinding direction on the characteristics of the surface of the prism plane sapphire. The results showed that the force was greater in the c-axis which was corresponding to the greatest surface damage. Wang et al. [22] proposed an analytical model for calculating the distribution of surface stress during grinding of bevel gear which was not developed in the previous models, taking into account the parameters of the process and two main factors to cause the surface residual stress, such as mechanical forces and grinding heat. Deng and Xu [23] reviewed and compared different methods of super-abrasive grinding wheel dressing in terms of efficiency, dressing accuracy, and processing cost. The review reported that, currently, the method of mechanical grinding wheel dressing is still the most used method because it is cheap, simple to operate, and mature technology. Dai et al. [24] developed a model of specific grinding force and specific energy taking into account the nonuniformity of the undeformed chip thickness. The results showed that the grinding specific force and energy increase with an increase of the percentage of active grains. Li et al. [25] established a methodology of grinding forces modeling considering the grinding parameters and the three stages of grit-workpiece interaction mechanism, such as rubbing, plowing, and cutting. The proposed methodology enabled determining the ratio of grains that are engaged in rubbing, plowing, and cutting. The methodology validated and provided a detailed information on grinding forces which was not addressed by the previous models. Lin et al. [26] proposed a model of surface roughness by analyzing the grit depth of cut model in ultrafine rotational grinding. The results showed that the chip formation, the cutting tip radius, and the effective number of grains have to be considered for grit depth of cut prediction.

Trung et al. [27] established the mathematical relationship between the surface roughness and the grinding forces. The authors revealed that the grinding forces depend on the grinding wheel parameters and the cutting parameters. Leonesio et al. [28] developed a simulation model of surface grinding to assess vibrations leading to the poor surface. The proposed model was able to predict the instability of the process related to the dynamic interaction between the machine and the process known as grinding chatter. Yang et al. [29] developed a model of the grinding regenerative chatter stability prediction to select the grinding parameters; the study showed that the wheel-workpiece interaction and the vibration coefficient are the main factors to limit the process chatter control. Cui et al. [30] presented a dynamic model for describing the wheel

and workpiece dynamics and to predict the generation of the workpiece roundness in the centreless grinding process. The developed model enabled predicting the workpiece roundness and providing the workpiece roundness error.

This work attempts to analyze the influence of the normal and tangential component of the grinding force resulting from the wheel-workpiece interaction mechanism on the vibration behavior of the flat surface grinding process through a nonlinear vibration modeling approach. Despite many significant models available in the literature predict grinding forces and dynamic stability of the grinding process, the model of correlation between the grinding forces and the vibration condition of the process needs to be investigated. In this work, a vibration model of the flat surface grinding process considering the grinding forces in the normal and tangential direction as the sources of the process vibration excitation is presented. To understand the changes of the process vibration behavior in normal and tangential direction due to the process parameters variation, the mathematical model of the tangential and normal component of grinding forces calculation developed in [10] was adopted in this study for the vibration model simulation. In the approach, the workpiece was considered to be rigid and the grinding wheel was modeled as a nonlinear two-degrees-of-freedom mass-spring-damper oscillator. In the following, the analysis of grinding forces is performed to develop its mathematical expression related to the vibration behavior first. The bifurcation diagram and the frequency response are then introduced to examine the vibration condition in the normal and tangential direction. Finally, a series of experimental tests are conducted to further validate the results of the process model simulation, and then discussions are made to explain different grinding modes.

2. Materials and Methods

2.1. Model of Flat Surface Grinding Process Vibration Excitation Forces. The total vibration excitation forces acting on the grinding system in the normal direction (F_n) and the tangential direction (F_t) are presented in Figure 1. Figure 1 also indicates the depth of cut (a), the rotational direction of the cutting speed (V_c), and the direction of the workpiece velocity (V_w). The forces acting on the grinding wheel and the workpiece are divided into two components, that is, the normal component and the tangential component of grinding forces. The total amount of cutting forces (F_T) acting on the system is obtained by a summation of forces in individual component expressed by

$$F_T = F_n + F_t. \quad (1)$$

2.2. Vibration Modeling of the Flat Surface Grinding Process. A free-body diagram of the flat surface grinding process with forces acting on the grinding wheel and the workpiece is indicated in Figure 2. There is a normal grinding force (N_1), which acts due to the chip formation, and a normal grinding force (N_2), which acts due to the friction between the wheel and the workpiece in the normal direction. There is a

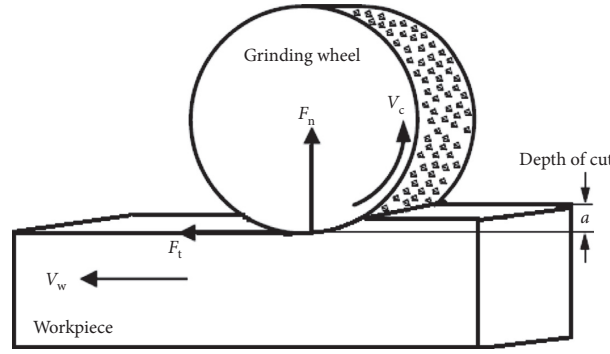

Figure 1: Schematic diagram of flat surface grinding vibration excitation forces.

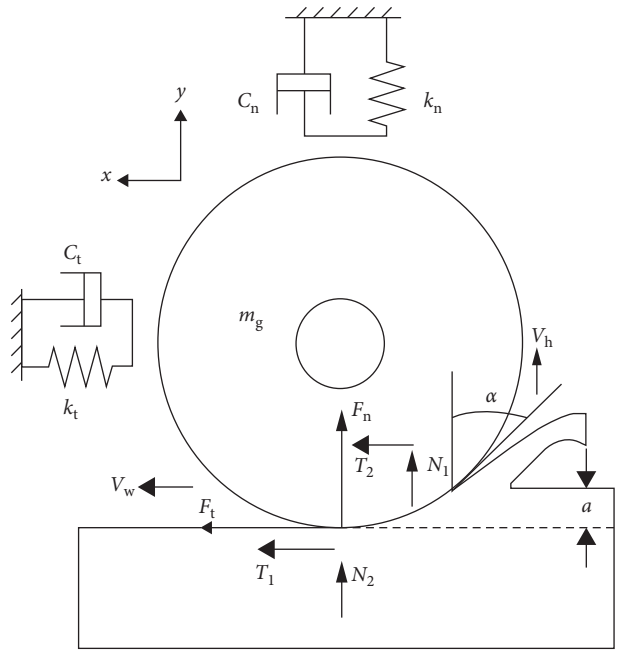

Figure 2: Free-body diagram of flat surface grinding vibration model.

grinding tangential force (T_1) acting due to the chip formation and a grinding tangential force (T_2) acting due to the friction between the grinding wheel and the workpiece in the tangential direction. The chip formation forces result from the interaction between the grinding wheel and the workpiece which is defined as a grit-workpiece interaction mechanism. The friction forces are generated by the friction between the workpiece and the grinding wheel which is classified into chip-bond, chip-workpiece, and bond-workpiece interaction mechanism, respectively.

The individual components of the normal and tangential grinding forces acting on the grinding wheel and the workpiece are replaced by their equivalent forces which are the tangential force (F_t) and the normal force (F_n), respectively, acting in two directions such as (F_t) in the horizontal direction corresponding to the x-axis parallel to the workpiece, and (F_n), acting in perpendicular direction corresponding to the y-axis perpendicular to the workpiece

as indicated in Figure 2. The two components of the resultant grinding forces from the chip formation and the friction between the grinding wheel and the workpiece, (F_t) and (F_n), can be calculated by summation of the grinding forces in both the tangential and the normal directions; that is,

$$\begin{cases} F_n = N_1 + N_2, \\ F_t = T_1 + T_2, \end{cases} \tag{2}$$

where N_1 is the normal chip formation force, N_2 is the normal friction force, T_1 is the tangential chip formation force, and T_2 is the tangential friction force, respectively.

The various forces acting on the grinding wheel and the workpiece need to be determined to complete the modeling of the flat surface grinding process. The grinding forces are determined as developed in [10]. For simplicity, the normal friction force and the tangential friction force are determined by the friction binomial theorem as follows:

$$\mu = \frac{\beta A_0}{P} + \alpha, \tag{3}$$

where μ indicates the coefficient of friction between the wheel and workpiece which govern the nonlinear characteristics of the friction forces between the wheel and the workpiece. A_0 is the area of wheel-workpiece contact, P is the normal grinding load, β is a coefficient determined by physical and mechanical properties of contact interface between the grinding wheel and the workpiece, and α is the rake angle of the abrasive grain.

The normal friction force (N_2) and the tangential friction force (T_2) are expressed by

$$\begin{cases} T_2 = bA\left(\beta + \dfrac{4\alpha p_0 V_w}{D_e V_c}\right)(D_e a)^{1/2}, \\ N_2 = \left(\dfrac{4bAp_0 V_w}{V_c}\right)\left(\dfrac{a}{D_e}\right)^{1/2}, \end{cases} \tag{4}$$

where D_e represents the grinding wheel equivalent diameter, a is the instantaneous depth of cut, p_0 is a constant to be experimentally determined, b is the width of the grinding wheel, A is the surface ratio of the wheel wear surface, V_w is the velocity of the workpiece, and V_c is the cutting speed.

The chip formation force in the tangential direction and the chip formation force in normal direction are determined according to the material of the workpiece, the material of the grinding wheel, and the parameters of the grinding process. Mathematically, the tangential chip formation force acting on the grinding wheel surface is expressed by a summation between the static tangential chip formation force and the dynamic cheap formation force as follows:

$$T_1 = \left(K_1 + K_2 \ln \frac{V_c^{1.5}}{a^{0.25} V_w^{0.5}}\right)\frac{V_w a}{V_c} b, \tag{5}$$

where K_2 represents a constant to be experimentally determined and K_1 indicates a summation of the static specific chip formation energy and the logarithm shear strain rate.

The normal chip formation force is expressed as follows:

$$N_1 = \left(\Phi_1 K_1 + \Phi_2 K_2 \ln \frac{V_c^{1.5}}{a^{0.25} V_w^{0.5}}\right)\frac{V_w a}{V_c} b, \tag{6}$$

where Φ_1 is the ratio between the static normal chip formation force to the static tangential chip formation force and Φ_2 is the ratio between the dynamic normal chip formation force to the dynamic tangential chip formation force.

As demonstrated in Figure 2, the grinding wheel along with its fixture assembly has been replaced by a two-degrees-of-freedom spring-mass-dashpot system. The grinding wheel can oscillate in tangential direction x (parallel to the workpiece) and normal direction y (perpendicular to the workpiece). The other various forces including the external forces acting on the process out of the x-y plane were neglected during the grinding process modeling. This verifies the two-degrees-of-freedom model for the combined machine grinding wheel process dynamics. In the flat surface grinding model, the grinding wheel is represented by a lumped mass (m_g) which can oscillate in the tangential x- and the normal y-directions. The interaction between the grinding wheel and the grinding wheel fixture assembly is represented by equivalent dashpot with damping coefficients c_t, c_n and equivalent springs with spring stiffness k_t, k_n in the tangential x- and normal y-directions, respectively. With the above simplifications, the governing equations of the grinding wheel motion in the flat surface grinding operation are mathematically expressed by the following ordinary differential equations:

$$\begin{cases} m_g \ddot{x} + c_t \dot{x} + k_t x = \left(K_1 + K_2 \ln \dfrac{V_c^{1.5}}{a^{0.25} V_w^{0.5}}\right)\dfrac{V_w a}{V_c} b + bA\left(\beta + \dfrac{4\alpha p_0 V_w}{D_e V_c}\right)(D_e a)^{1/2}, \\ m_g \ddot{y} + c_n \dot{y} + k_n y = \left(\Phi_1 K_1 + \Phi_2 K_2 \ln \dfrac{V_c^{1.5}}{a^{0.25} V_w^{0.5}}\right)\dfrac{V_w a}{V_c} b + \left(\dfrac{4bAp_0 V_w}{V_c}\right)\left(\dfrac{a}{D_e}\right)^{1/2}. \end{cases} \tag{7}$$

The instantaneous depth of cut (a) resulting from the wheel vibrations can be written in terms of the specified depth of cut (a_0) and the grinding wheel vibration displacement motion in the normal direction y as follows:

$$a = a_0 - y. \tag{8}$$

The relative velocities between the grinding wheel and the workpiece (V_w) and the grinding wheel and the chip (V_h) are related to the nominal cutting speed V_c, the rake angle α, and the grinding wheel velocities $\dot{x}$ and $\dot{y}$ by

$$\begin{aligned} V_w &= V_c - \dot{x}, \\ V_h &= V_w \tan\alpha - \dot{y}. \end{aligned} \tag{9}$$

$\tan\alpha$ is resulting from the variation of the grit geometry due to grit wear which generates the change of the chip thickness from the grinding process and the thickness of the workpiece material approaching the grinding wheel.

The nondimensional equations of motion are obtained by using a characteristic time scale determined by the natural frequency of vibration in normal and tangential direction mathematically expressed as

$$\begin{cases} \ddot{x} + 2s_t\dot{x} + x = F_t, \\ \ddot{y} + 2s_n\sqrt{\xi}\,\dot{y} + \xi y = F_n, \end{cases} \tag{10}$$

where $\xi = k_n/k_t$ is the stiffness ration; $w_t^2 = k_t/m_g$ is the natural frequency in tangential direction; $w_n^2 = k_n/m_g$ is the natural frequency in normal direction; $s_t = c_t/2m_g w_t$ is the damping ration in tangential direction; and $s_n = c_n/2m_g w_n$ is the damping ration in normal direction.

2.3. Experimental Procedure. The flat surface grinding process is a complex phenomenon that involves various factors to influence its nonlinear vibrations. Specifically, the complexity of the process is found in its mode of grinding wheel-workpiece interaction which involves grit-workpiece, chip-bond, chip-workpiece, and bond-workpiece interactions, respectively. The grit-workpiece interaction is the only one to accomplish the cutting action and remove the material on the workpiece in form of a chip. The other three are undesirable because they increase the power and forces required during the process, but they are inevitable in the real grinding process. Furthermore, the complexity of the process lies in the grit-workpiece contact zone such as rubbing, plowing, and shearing. Grinding forces are considered as the major factor of process vibration excitation. Mathematical analysis and model simulation methods can not accurately predict the vibration condition of the process because they do not consider various external factors which can influence the vibration behavior of the process. To gain a proper insight into the vibration condition of the flat surface grinding process, an experimental campaign of grinding force measurement and force signals conversion into frequency domain was adopted as a concise method of the nonlinear vibration condition prediction.

2.4. Experimental Setup. The experiments for grinding force measurements were performed on a flat surface grinding machine of Chevalier FSG2A818 type. The grinding operation was accomplished by the use of the aluminum oxide grinding wheel with resin bonding type and with code 7A36IBJ15. The wheel dimensions are $400 \times 57 \times 127$ mm which means the external diameter of 400 mm, the width of 57 mm, and the inner diameter of 127 mm, respectively. During grinding, grit wear can induce higher grinding force and higher temperature in the grinding zone. To keep the wheel sharpness and grit size, the mechanical dressing method was adopted [23]. Before each series of the experiment, the grinding wheel was dressed by a multigrit diamond dressing tool with the dressing depth of 0.03 mm. The schematic diagram of the experimental setup is indicated in Figure 3.

The workpiece material was mild steel (BS970 080440) with an average hardness of about 90 HRB and of dimensions $250 \times 200 \times 50$ mm which means 250 mm of length, 200 mm of width, and 50 mm of thickness, respectively. The mild steel is commonly used in construction applications and is made up of iron and carbon, with relatively much more iron content which makes it very strong and easy to be machined. The workpiece material parameters are presented in Table 1.

In each experimental test, the components of the grinding force values and signals were obtained. The measurements of normal (F_n) and tangential (F_t) components of grinding force were done by the use of a 3-component dynamometer type 9257 A with a measurement of about 5000 N in x-, y-, and z-axis. The cutting force signals from the dynamometer were amplified by a charge amplifier of type 5019 A (Kistler Holding AG, Switzerland). The obtained data from the dynamometer were recorded using a data acquisition system of type National Instruments NI-6250 data acquisition (DAQ) card with 8 analog inputs (16 bits) ADC resolution at the sampling frequency of 2 MHz. To reduce the effect of noise level in and out of the process, a converter of type 5125B2 (Kistler Holding AG, Switzerland) with the low-pass filter ranging from 0.3 kHz to 10 kHz was used to convert the analog signals of forces. The acquired force data signals were recorded on PC and analyzed with the help of DynoWare software. To further process the grinding force data, MATLAB and Excel software were used. The experiments were carried out in up and dry grinding setup conditions, and each experimental test was repeated four times to ensure the accuracy of the results. The experimental data are presented in Table 2.

3. Results and Discussion

3.1. Vibration Condition Analysis of the Flat Surface Grinding Process. In this section, the numerical simulation method is used to investigate the nonlinear vibration condition of the grinding wheel in the flat surface grinding process. The bifurcation diagrams of the mathematical analyses of the flat surface grinding process presented in Section 2 are performed in MATLAB. The vibration characteristics of the process versus the depth of cut a_0 and the cutting speed V_c were obtained through the appropriate bifurcation diagrams presented in Figures 4–6.

A set of nondimensional parameters was adopted to obtain these bifurcations; that is, $a_0 = 0.02$, $V_c = 0.3$, $\xi = 1$, $\beta = 0.1$, $\mu = 0.3$, $\alpha = 45^\circ$, and $A = 0.5$.

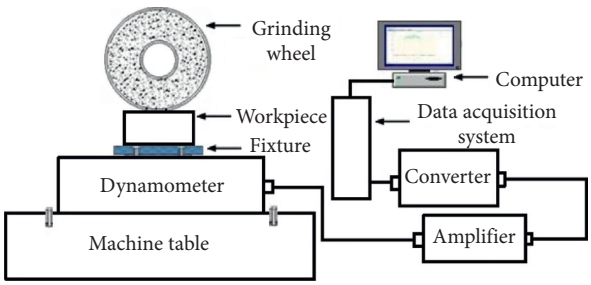

Figure 3: Schematic diagram of the experimental setup.

Table 1: The workpiece material parameters.

Material	Unit	Mild steel
Mass density	(kg/m^3)	7850
Thermal expansion coefficient	($^\circ$C^{-1})	$1.2 * 10^{-5}$
Young's modulus	(MPa)	$2 * 10^5$
Thermal conductivity	(W/mK)	60.5
Specific heat	(J/kgK)	434
Poisson's ration		0.3

The bifurcation diagrams were constructed by plotting the vibration amplitude of the grinding wheel on the vertical axis versus the depth of cut on the horizontal axis in normal and tangential directions. In the flat surface grinding process, the cutting speed (V_c) and the depth of cut (a) are significant parameters that directly affect the vibration condition and the quality production of the process. Therefore, the depth of cut and the cutting speed were adopted as the bifurcation parameters.

The bifurcation diagram presented in Figure 4 shows a higher growth of vibration amplitudes in the normal direction than in the tangential direction. In the tangential direction, vibrations are practically constant as indicated in Figure 4(a), while in the normal direction, Figure 4(b) indicates the growth of the vibration amplitude. The tangential component of the grinding forces mainly affects the power consumption by the friction between the grinding wheel and the workpiece. Hence, the tangential component of the grinding system shows fewer vibrations. However, the normal component shows the growth of vibrations due to its influence on material removal. The grit-workpiece engagement introduces more cutting forces in normal component than in the tangential component to induce more vibrations in the normal component of the process. The bifurcation diagram results express that, at the cutting speed of 20 m/s, vibrations are lower in tangential direction than in the normal direction.

The vibration conditions of the grinding system at the cutting speed of 25 m/s presented in Figure 5 indicate that there is a linear relationship between the dynamic instability of the flat surface grinding process and the rise of the cutting speed. The increases in the cutting speed cause an increase of the nonlinear vibration behavior of the process in both normal and tangential directions. For the normal direction, Figure 5(b) indicates an obvious increase in the amplitudes of vibration. For the tangential direction, Figure 5(a) presents a slight increase in the amplitude of vibrations compared to the normal direction. In normal and tangential directions, the process shows fluctuations. At this level, the increase of the cutting speed and the depth of cut leads to the increase of the vibration excitation cutting forces due to the increase of material removal rate and the cross-section area of the material removal. There is a linear relationship existing between the uncut chip thickness and the vibration excitation cutting forces. This is in agreement with the well-known statement in the metal cutting process that, a rise of the cutting speed and the depth of cut results in more vibrations. But due to a nonlinear interaction between the grinding wheel and the workpiece, an increase of the cutting speed and the depth of cut to some extent can improve the stability of the process. The results of the system vibration condition suggest that at the cutting speed of 25 m/s the vibrations grow in both normal and tangential directions, but they grow very quickly in the normal component of the process than the tangential component.

The results of the bifurcation diagram for the grinding system vibration conditions presented in Figure 6 indicate that, at the cutting speed of 30 m/s, the amplitudes of vibration of the grinding wheel in the tangential direction continue to increase, while the opposite is observed in the normal direction because the amplitudes of vibration in the normal direction decrease gradually. At the cutting speed of 30 m/s, the vibrations become larger in the tangential direction and diminish significantly in the normal direction.

According to the flat surface grinding process vibration model presented in Figure 2, the tangential component of the grinding force is introduced by the effect of friction between the grinding wheel and the workpiece. The rise of the cutting speed and the depth of cut enhances the wheel-workpiece friction mechanism due to a large cross-section area of the workpiece material removal and leads to the increase of vibration instability level in the tangential component of the process.

The normal component of the grinding forces is generally translated into cutting action by grit penetration into the workpiece material as indicated in Figure 2. For some workpiece material known as easy to grind materials, such as various steels commonly used in manufacturing applications, the large wheel-workpiece friction generates more amount of heat which leads to the workpiece material thermal softening. The thermal softening effect cause the workpiece material to be easily cut which reduce the normal cutting forces and decrease the level of vibration instability in the normal component of the process.

This corresponds to the improved dynamic stability of the flat surface grinding process because the normal direction corresponds to the normal component of grinding force which has a great influence on the dynamic stability of the flat surface grinding process.

The cutting speed (V_c) and the depth of cut (a) are the key parameters of the flat surface grinding process to influence the system dynamics and to affect the quality of the ground part. Reducing the depth of cut can be one of the simplest ways of controlling and suppressing vibrations in the flat surface grinding process, but it will significantly increase the machining time because of low material removal

Table 2: Experimental input parameter and values of measured grinding forces.

Test	V_w (mm/min)	a (mm)	V_c (m/s)	$F_t(N)$	$F_n(N)$	Grinding condition
1	400	0.005	20	18.3	41.6	
2	400	0.01	25	35.7	107.1	Up/dry
3	400	0.02	30	28.6	74.9	

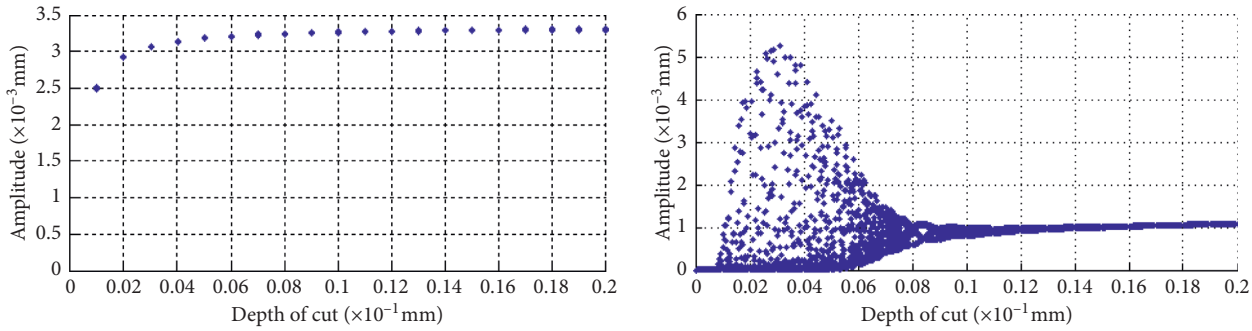

Figure 4: Bifurcation diagram of the grinding wheel displacement as a function of the depth of cut at the cutting speed of 20 m/s. (a) Tangential direction. (b) Normal direction.

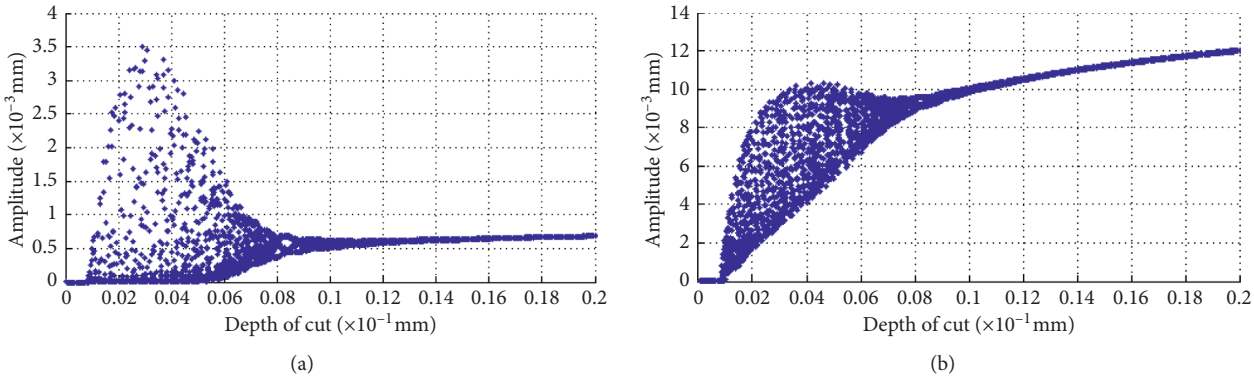

Figure 5: Bifurcation diagram of the grinding wheel displacement as a function of the depth of cut at the cutting speed of 25 m/s. (a) Tangential direction. (b) Normal direction.

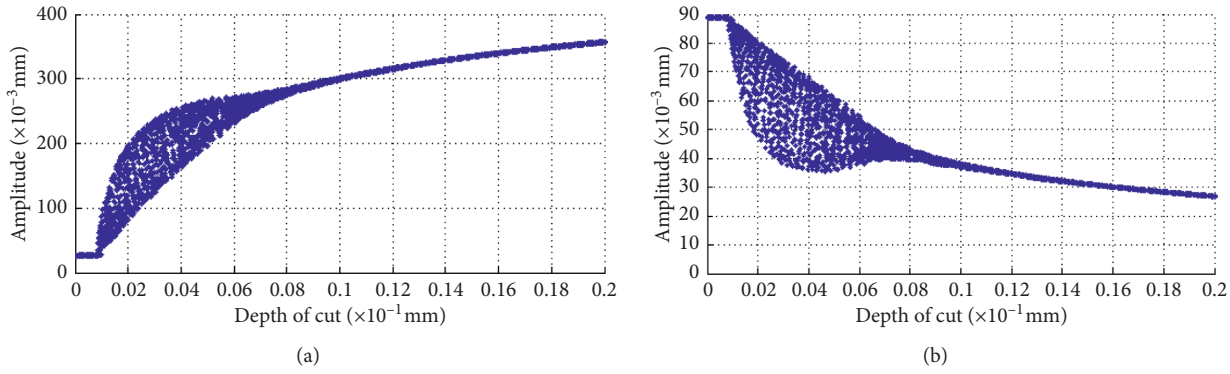

Figure 6: Bifurcation diagram of the grinding wheel displacement as a function of the depth of cut at the cutting speed of 30 m/s. (a) Tangential direction. (b) Normal direction.

rate. The bifurcation diagrams presented in Figures 4–6 demonstrate that the alteration of the cutting speed and the depth of cut affects differently the tangential and the normal component of the grinding process in terms of vibration conditions. For the tangential component of the process, increasing the cutting speed and the depth of cut is

accompanied by a rise of the amplitudes of vibration. In the normal component of the process, for the cutting speed (V_c) ranging from 20 to 25 m/s, increasing the depth of cut (a) destabilize the dynamics of the process, while the reverse is observed at the cutting speed of 30 m/s because the vibration diminishes gradually at the cutting speed of 30 m/s and the depth of cut of 0.02 mm. From the practical point of view, the normal component of the flat surface grinding process plays a major role in the vibration behavior of the grinding process, which means smaller vibration in the normal component characterizes improved dynamic stability of the grinding process. This implies that grinding at the cutting speed of 30 m/s will allow cutting at the depth of cut of 0.02 mm and reduce the time of grinding without compromising the grinding stability.

3.2. Experimental Verification. This experimental work deals with the analysis of the variation in vibration condition of the flat surface grinding process by taking into consideration the depth of cut and the cutting speed as the parameters to induce the process vibration instability by the action of grinding forces. The literature has reported the effect of the cutting speed and the depth of cut on the variation of cutting forces; however, it was not clear whether the cutting speed and the depth of cut can affect the process dynamic stability. The vibration condition in the normal and tangential direction needs to be investigated. Therefore, the values of the input parameters in the experiments were adopted with the idea of minimizing the process vibration instability such as the cutting speed as reported in [31], depth of cut as developed in [12, 14], and workpiece speed (feed rate) as stated in [32, 33].

To understand the influence of change of grinding parameters on the vibration condition of the process in the normal and tangential directions, the fast Fourier transform (FFT) has been used to process and transform each grinding force component-time history signals into the frequency-domain plots presented in Figures 7–9. The vertical axis indicates the amplitude of vibrations, and the horizontal axis indicates the frequency of vibrations. The results of the frequency domain corresponding to the time history of dynamic cutting force signals measured at 0.005 mm depth of cut, 20 m/s cutting speed, and 400 mm/min workpiece velocity (table speed) are presented in Figure 7. The frequency-domain plot of the tangential direction is indicated in Figure 7(a) and presents no significant peak which means fewer fluctuations of the process in the tangential direction. The frequency domain in the normal direction of the process is presented in Figure 7(b). The frequency-domain plot of the normal component shows significant peaks, which mean more fluctuation in the normal component of the process compared to the tangential component of the process. The more fluctuations in the normal component are due to its greater contribution in the chip formation during the grinding process to induce more vibration excitation forces. The normal component of the grinding forces is mostly caused by the workpiece resistance to grit penetration for material removal, while the tangential component mainly contributes to the wheel-workpiece friction mechanism, hence the fewer vibration excitation forces in the tangential component. This agrees with the simulation results obtained in Figure 4, which mentioned that vibrations are lower in the tangential direction than in the normal direction of the flat surface grinding process.

The experimental results of the frequency domain for the measured grinding forces signals at 0.01 mm depth of cut, 25 m/s cutting speed, and 400 mm/min workpiece velocity are presented in Figure 8. The grinding vibration conditions in both normal and tangential directions are presented by the frequency-domain plots. A significant change is realized in the vibration condition of the process for the normal and the tangential component. The increase of the cutting speed and the depth of cut has led to an increase of the vibrations in the tangential and the normal directions as indicated in Figures 8(a) and 8(b). This is due to the increase of the grain penetration into the workpiece which means a rise of the depth of cut, to generate bigger undeformed chip thickness and much more material removal that cause an increase in grinding forces to induce more vibrations of the process. In the frequency-domain plot presented in Figure 8(b) an obvious increase of the vibrations in the normal direction is observed. This indicates that the normal component of the process has more effect on the dynamic stability of the process. The frequency-domain plot shown in Figure 8(a) indicates that the vibration behavior has not significantly changed in the tangential direction. This means that the tangential component of the flat surface grinding process is less sensitive than the normal component to the increase of the cutting speed and the depth of cut. The obtained experimental results approve the simulation results obtained in Figure 5 indicating that by increasing the cutting speed and the depth of cut, vibrations grow more quickly in normal direction than in the tangential direction.

The frequency domain of the obtained dynamic grinding force signals at 0.02 mm depth of cut, 30 m/s cutting speed, and 400 mm/min workpiece velocity is indicated in Figure 9. The frequency domain in the normal component of the process indicated in Figure 9(b) expresses that the increase of the cutting speed and the depth of cut parameters can reduce the vibrations and the grinding forces [34]. The corresponding frequency response plot for the normal component of the system is characterized by a single peak, which signifies fewer vibrations. The amplitudes and the frequency of vibrations have reduced significantly compared to the frequency and amplitudes of vibrations for the normal component indicated in Figure 8(b). This shows that the increase in the cutting speed has a stabilizing effect on the grinding system vibration condition.

In the tangential component of the flat surface grinding system presented in Figure 9(a), the reverse to the normal component is observed. The rise in the cutting speed and the depth of cut is associated with a slight increase of vibration amplitudes and frequency in the tangential direction.

This is due to the effect of the workpiece material and the mechanism of wheel-workpiece interaction which includes the material removal phenomenon in form of chips and the friction phenomenon which generates the amount of heat in

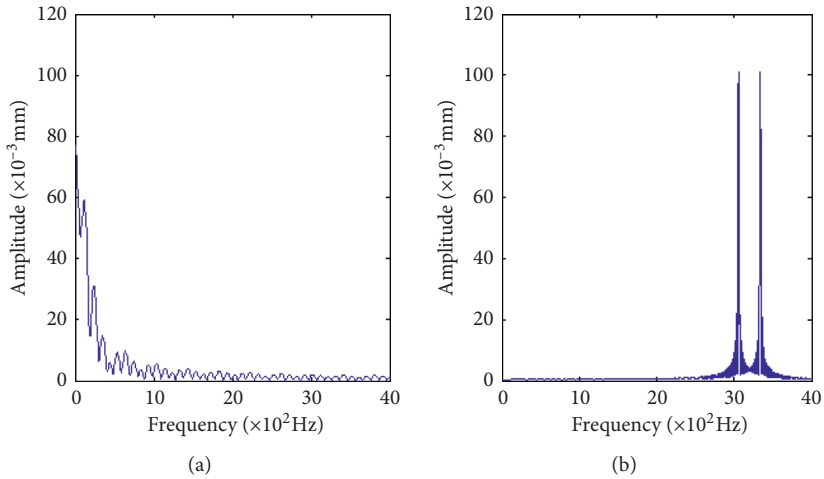

Figure 7: Frequency domain of the dynamic cutting forces at the depth of cut (a = 0.005 mm), cutting speed (V_c = 20 m/s), and workpiece velocity V_w = 400 mm/min. (a) Tangential component. (b) Normal component.

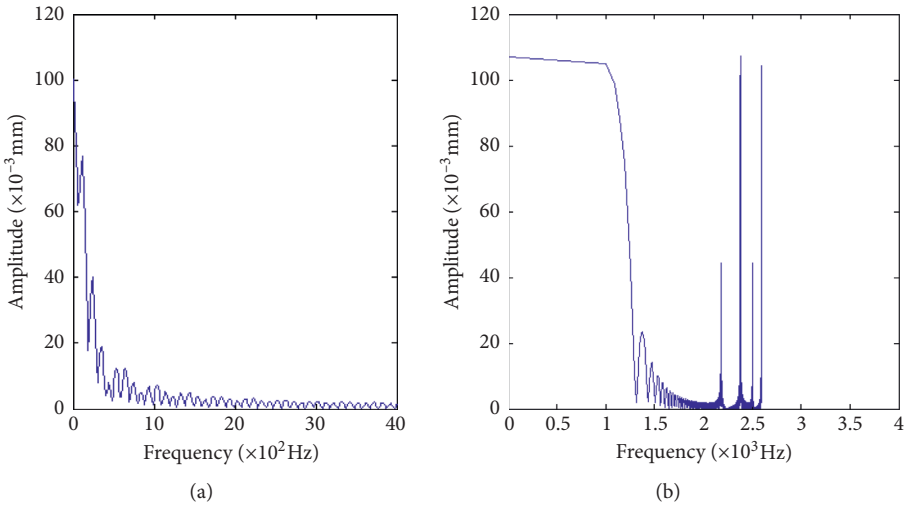

Figure 8: Frequency-domain of the dynamic cutting forces at the depth of cut (a = 0.01 mm), cutting speed (V_c = 25 m/s), and workpiece velocity V_w = 400 mm/min. (a) Tangential component. (b) Normal component.

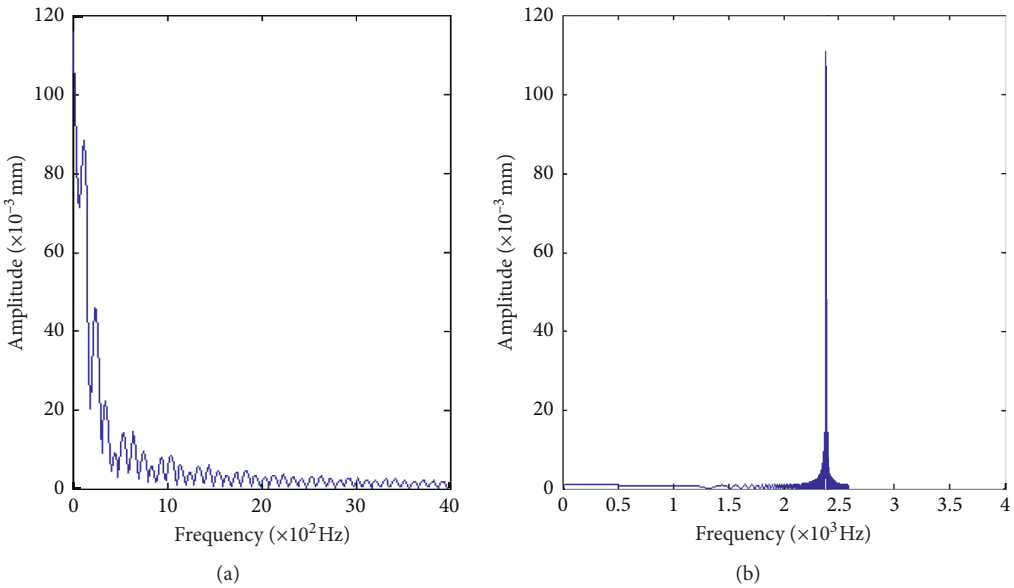

Figure 9: Frequency domain of the dynamic cutting forces at the depth of cut (a = 0.02 mm), cutting speed (V_c = 30 m/s), and workpiece velocity V_w = 400 mm/min. (a) Tangential component. (b) Normal component.

the wheel-workpiece contact zone. Further increase of the cutting speed at 30 m/s and the depth of cut at 0.02 mm introduces more wheel-workpiece friction to generate more tangential excitation forces to induce more vibrations in the tangential component of the system. On the other hand, the heat generated from friction in the wheel-workpiece contact zone causes the thermal softening of the workpiece material especially for the easy-to-grind materials such as the mild steel used in the experimental test. The thermal softening behavior causes the workpiece material to be easily removed. This reduces the normal excitation forces and improves the dynamic stability of the process in the normal component.

The results presented in Figure 9 verify the simulation results obtained in Figure 6; that is, at the cutting speed of 30 m/s and the depth of cut of 0.02 mm, the vibrations increase in the tangential direction and diminish in the normal direction.

The results of the experiments for the flat surface grinding process vibration conditions and force measurement have demonstrated that the higher values of grinding forces were obtained in the normal component (see Table 2) which concurs with the previous research findings in the literature [27, 35]. It can be noted that, in the range of the cutting speed from 20 to 25 m/s and the depth of cut from 0.005 to 0.01 mm, the increase of the cutting speed and the depth of cut parameters is connected with an increase in the grinding forces and the amplitudes of vibration in both tangential and normal directions, but the grinding forces and vibrations grow more quickly in normal direction than in the tangential direction. However, at the cutting speed of 30 m/s and depth of cut of 0.02 mm, the grinding forces and vibrations reduce significantly in the normal direction and increase slightly in the tangential direction. In the practical point of view, the cutting speed of 30 m/s results in improved dynamic stability of the flat surface grinding and can permit grinding at the depth of cut of 0.02 mm without sacrificing the stability of the process since the normal component has greater influence than the tangential component in the vibration condition of the process.

4. Conclusion

In this paper, an analytical comparison of the influence of the normal and the tangential component on the vibration condition of the flat surface grinding process was investigated by the bifurcation diagram method. The analytical model incorporated grinding parameters including the depth of cut and the cutting speed. The effect of these parameters on the change of the vibration behavior of the process has been examined. The experiments of the flat surface grinding process were carried out to study grinding forces variation and process vibration conditions to validate the results of the vibration model. The results show that the change of depth of cut and the cutting speed induces a nonlinear dynamic behavior of the process, and the normal component makes a greater contribution than the tangential component in the vibration condition of the process. For the grinding parameters, the cutting speed of 30 m/s can allows cutting at the depth of cut of 0.02 mm without compromising the dynamic stability of the process. With the developed model, further study can be carried out to learn the effect of other parameters such as machine dynamics parameters and grinding wheel topography parameters.

Notations

A: Surface ratio of the wheel wear surface
A_0: Area of wheel-workpiece contact
b: Width of the grinding wheel
c_n: Damping coefficient in normal direction
c_t: Damping coefficient in tangential direction
D_e: Grinding wheel equivalent diameter
F_T: Total grinding force
F_n: Normal grinding force component
F_t: Tangential grinding force component
a: Instantaneous depth of cut
a_0: Nominal depth of cut
K_1: Static specific chip formation energy and the logarithm shear strain rate summation
K_2: Constant to be determined experimentally
k_n: Equivalent spring stiffness in normal direction
k_t: Equivalent spring stiffness in tangential direction
m_g: Mass of the grinding wheel
N_1: Normal chip formation force
N_2: Normal friction force
P: Normal grinding load
p_0: Constant to be determined experimentally
s_t: Damping ration in tangential direction
s_n: Damping ration in normal direction
T_1: Tangential chip formation force
T_2: Tangential friction force
V_h: Relative velocity between the grinding wheel and the chip
V_c: Cutting speed
V_w: Velocity of the workpiece
w_t: Natural frequency in tangential direction
w_n: Natural frequency in normal direction
α: Rake angle of the abrasive grain
β: Wheel and the workpiece physical and mechanical contact interface properties
μ: Coefficient of friction
ξ: Stiffness ration
Φ_1: Ratio between the static normal chip formation forces to the static tangential chip formation force
Φ_2: Ratio between the dynamic normal chip formation forces to the dynamic tangential chip formation force.

Data Availability

The data used to support the findings of this study are available from the corresponding author upon request.

Conflicts of Interest

The authors declare that there are no conflicts of interest regarding the publication of this paper.

Acknowledgments

The authors acknowledge the support of the School of Mechanical and Electronic Engineering, Lanzhou University of Technology and the Rwanda Polytechnic-Integrated Polytechnic Regional College-Kigali (IPRC-Kigali). This work has been supported by the National Natural Science Foundation of China (Grant no. 11372122) and the Science and Technology Program of Gansu Province of China (Grant no. 1610RJYA020).

References

[1] G. Yin and D. Marinescu, "A heat transfer model of grinding process based on energy partition analysis and grinding fluid cooling application," *ASME Journal of Manufacturing Science and Engineering*, vol. 139, no. 12, 2017.

[2] R. Kountanya and C. Guo, "Force and temperature modeling in 5—axis grinding," *Procedia Manufacturing*, vol. 26, pp. 521–529, 2018.

[3] S. Malkin, *Theory and Application of Machining with Abrasives Grinding Technology*, Ellis Horwood Limited, Hemel Hempstead, UK, 1989.

[4] C. Bhateja and R. Lindsay, *Techniques and Troubleshooting Grinding Theory*, Society of Manufacturing Engineers, Dearborn, MI, USA, 1992.

[5] S. Malkin, *"Grinding Technology Theory and Applications of Machining with Abrasives*, Society of Manufacturing Engineers, Dearborn, MI, USA, 1989.

[6] R. S. Hahn, *On the Nature of the Grinding Process*, Pergamon Press, Birmingham, UK, 1962.

[7] S. Hahn and L. Robert, *Principles of Grinding: Theory, Techniques and Troubleshooting*, Society of Manufacturing Engineers, Dearborn, MI, USA, 1971.

[8] R. P. Lindsay and R. S. Hahn, "On the basic relationships between grinding parameters," *Annals of the CIRP*, vol. 18, pp. 657–666, 1971.

[9] R. P. Lindsay, "Principles of grinding," *Handbook of Modern Grinding Technology*, pp. 30–71, Chapman & Hall, London, UK, 1986.

[10] J. Tang, J. Du, and Y. Chen, "Modeling and experimental study of grinding forces in surface grinding," *Journal of Materials Processing Technology*, vol. 209, no. 6, pp. 2847–2854, 2009.

[11] P. Durgumahanti, V. Singh, and V. Rao, "A new model for grinding force prediction and analysis," *International Journal of Machine Tools & Manufacture*, vol. 50, no. 3, pp. 231–240, 2010.

[12] H.-C. Chang and J.-J. J. Wang, "A stochastic grinding force model considering random grit distribution," *International Journal of Machine Tools and Manufacture*, vol. 48, no. 12-13, pp. 1335–1344, 2008.

[13] V. K. Mishra and K. Salonitis, "Empirical estimation of grinding specific forces and energy based on a modified werner grinding model," *Procedia CIRP*, vol. 8, pp. 287–292, 2013.

[14] K. Salonitis, P. Stavropoulos, and A. Kolios, "External grind-hardening forces modelling and experimentation," *The International Journal of Advanced Manufacturing Technology*, vol. 70, no. 1–4, pp. 523–530, 2014.

[15] J. Jiang, P. Ge, S. Sun, D. Wang, Y. Wang, and Y. Yang, "From the microscopic interaction mechanism to the grinding temperature field: an integrated modelling on the grinding process," *International Journal of Machine Tools and Manufacture*, vol. 110, pp. 27–42, 2016.

[16] Q. Liu, X. Chen, Y. Wang, and N. Gindy, "Empirical modelling of grinding force based on multivariate analysis," *Journal of Materials Processing Technology*, vol. 203, no. 1–3, pp. 420–430, 2008.

[17] Y. Wang, D. Guangheng, J. Zhao et al., "Study on key factors influencing the surface generation in rotary ultrasonic grinding for hard and brittle materials," *Journal of Manufacturing Processes*, vol. 38, pp. 549–555, 2019.

[18] Y. Wang, X. Chu, Y. Huang, G. Su, and D. Liu, "Surface residual stress distribution for face gear under grinding with a long-radius disk wheel," *International Journal of Mechanical Sciences*, vol. 159, pp. 260–266, 2019.

[19] W.-L. Zhu, Y. Yang, H. N. Li, D. Axinte, and A. Beaucamp, "Theoretical and experimental investigation of material removal mechanism in compliant shape adaptive grinding process," *International Journal of Machine Tools and Manufacture*, vol. 142, pp. 76–97, 2019.

[20] W. Yuqin, J. Tang, Z. Wei, and C. Zhu, "Study on contact performance of ultrasonic-assisted grinding surface," *Ultrasonics*, vol. 91, pp. 193–200, 2019.

[21] W. Zhao, Y. Wang, Z. Liang et al., "Research on ground surface characteristics of prism-plane sapphire under the orthogonal grinding direction," *Applied Surface Science*, vol. 489, pp. 802–814, 2019.

[22] Y. Wang, W. Zhang, and Y. Liu, "Analysis model for surface residual stress distribution of spiral bevel gear by generating grinding," *Mechanism and Machine Theory*, vol. 130, pp. 477–490, 2018.

[23] H. Deng and Z. Xu, "Dressing methods of superabrasive grinding wheels: a review," *Journal of Manufacturing Processes*, vol. 45, pp. 46–69, 2019.

[24] C. Dai, Z. Yin, W. Ding, and Y. Zhu, "Grinding force and energy modeling of textured monolayer CBN wheels considering undeformed chip thickness nonuniformity," *International Journal of Mechanical Sciences*, vol. 157-158, pp. 221–230, 2019.

[25] H. N. Li, T. B. Yu, Z. X. Wang, L. D. Zhu, and W. S. Wang, "Detailed modeling of cutting forces in grinding process considering variable stages of grain-workpiece micro interactions," *International Journal of Mechanical Sciences*, vol. 126, pp. 319–339, 2017.

[26] B. Lin, Z. Wang, Y. Yan, P. Zhou, R. Kang, and D. Guo, "Analytical elastic–plastic cutting model for predicting grain depth-of-cut in ultrafine grinding of silicon wafer," *Journal of Manufacturing Science and Engineering*, vol. 140, no. 12, pp. 1–7, 2018.

[27] D. Trung, N. Man, and P. Son, "Determining cutting force after surface roughness measurement in grinding," *Advances in Engineering Research and Application*, vol. 63, pp. 1–7, Springer, Cham, Switzerland, 2019.

[28] M. Leonesio, P. Parenti, A. Cassinari, G. Bianchi, and M. Monno, "A time-domain surface grinding model for dynamic simulation," *Procedia CIRP*, vol. 4, pp. 166–171, 2012.

[29] Y. Yang, J. Lin, and S. Xu, "Surface grinding machine stability characteristics limited prediction," *Mechanical Engineering Research*, vol. 2, no. 2, 2012.

[30] Q. Cui, H. Ding, and K. Cheng, "An analytical investigation on the workpiece roundness generation and its perfection strategies in centreless grinding," *Proceedings of the Institution of Mechanical Engineers, Part B: Journal of Engineering Manufacture*, vol. 229, no. 3, pp. 409–420, 2014.

[31] Y. X. Jiang, W. X. Tang, G. L. Zhang, Q. H. Song, B. B. Li, and B. Du, "An experiment investigation for dynamics characteristics of grinding machine," *Key Engineering Materials*, vol. 329, pp. 767–772, 2007.

[32] V. Francis, A. Khalkho, and J. Tirkey, "Experimental investigation and prediction of surface roughness in surface grinding operation using factorial method and regression analysis," *International Journal of Mechanical Engineering and Technology*, vol. 5, pp. 108–114, 2014.

[33] I. V. Tsiakoumis, "An investigation into vibration assisted machining—application to surface grinding processes," Doctoral thesis, Liverpool John Moores University, Liverpool, UK, 2011.

[34] X. Li, "Modeling and simulation of grinding processes based on a virtual wheel model and microscopic interaction analysis," Doctoral thesis, Worcester Polytechnic Institute, Worcester, MA, USA, 2010.

[35] W. Habrat, M. Żółrat, J. Ś.łrat, and E. Socha, "Forces modeling in a surface peripheral grinding process with the use of various design of experiment (DoE)," *Mechanik*, vol. 91, no. 10, pp. 929–931, 2018.